

# Compact Smart Antenna With Electronic Beam-Switching and Reconfigurable Polarizations

Chao Gu, Steven Gao, Haitao Liu, Qi Luo, Tian-Hong Loh, Mohammed Sobhy, Jianzhou Li, Gao Wei, Jiadong Xu, Fan Qin, B. Sanz-Izquierdo, and Raed A. Abd-Alhameed

***Abstract*—This paper presents a compact-size, low-cost smart antenna with electronically switchable radiation patterns, and reconfigurable polarizations. This antenna can be dynamically switched to realize three different polarizations including two orthogonal linear polarizations and one diagonally linear polarization. By closely placing several electronically reconfigurable parasitic elements around the driven antenna, the beam switching can be achieved in any of the three polarization states. In this design, a polarization reconfigurable square patch antenna with a simple feeding network is used as the driven element. The parasitic element is composed of a printed dipole with a PIN diode. Using different combinations of PIN diode ON/OFF states, the radiation pattern can be switched toward different directions to cover an angle range of 0° to 360° in the azimuth plane. The concept is confirmed by a series of measurements. This smart antenna has the advantages of compact size, low cost, low power consumption, reconfigurable polarizations, and beams.**

***Index Terms*—Beam switching, pattern diversity, polarization diversity, reconfigurable antenna, smart antenna.**

## I. Introduction

ANTENNA diversity is an effective technique of mitigating multipath fading and enhancing the performance of wireless systems. Antenna diversity can be divided into space diversity, polarization diversity, and radiation pattern diversity.

Several polarization diversity antennas were reported and these antennas are useful for reducing the polarization mismatches that could cause poor signal reception [1]–[5]. The best signal strength can be achieved by dynamically altering the polarizations to match the polarization states of the received signals. Radiation pattern diversity is used to introduce space division multiple access (SDMA) network architecture into communication systems to increase the channel capacity. Furthermore, the radiation pattern switching ability can suppress the cochannel interference and increase the link margin significantly. Since wireless channels are time variant, the employed polarization and radiation pattern scheme should be updated in real time.

Phased arrays and digital beamforming (DBF) arrays are two well-known techniques of realizing beam-switching antennas. Phased arrays require a large number of microwave phase shifters while DBF requires a large number of RF amplifiers, mixers, and analogue-to-digital converters (ADC). Hence both techniques lead to a smart antenna with a bulky size, high cost and high power consumption. It is also possible to realize beam-switching antennas using multibeam feed networks such as Butler matrix. However, such beam-forming networks (e.g., Butler matrix) are large in size and lossy, thus leading to large size of smart antennas. Therefore, more research is required to find new solutions to compact-size, low-cost smart antennas.

In the past decade, electronically steerable parasitic array radiator (ESPAR) antennas have received increasing research interests due to the advantages of low cost and low power consumption [6]–[12]. An ESPAR antenna consists of one driven element and several parasitic elements with reactive or resistive loads. It is not necessary to use phase shifters and only one driven element is connected to the RF front end. Moreover, the beamforming elements in an ESPAR antenna do not require feeding networks, which reduces the complexity of antenna array design. Signals received by the parasitic elements are fed into the driven element by electromagnetic coupling. The received signal is down converted in the mixer and digitized by an ADC. The digitized signals are then fed into the transceiver. The surface currents induced on the parasitic elements can be controlled by the impedance of the PIN diodes [6] or the capacitance of the varactors [11]. By controlling the dc voltages applied to these components, the induced surface current can be controlled and thus the antenna radiation pattern can be steered.

Polarization reconfigurable antennas were investigated in [13]–[16]. Most of these antennas can achieve dynamic polarization switching, e.g., from linear polarizations to circular polarizations. Compared to the conventional dual polarization antennas presented in [17]–[19], reconfigurable antennas are more attractive due to reduced hardware complexity and efficient utilization of power and electromagnetic spectrum. However, the beams of the proposed antennas in [13]–[16] cannot be steered. The dual port antenna in [3] generates two fixed beams to perform pattern diversity, which is not suitable for beam switching applications. In [20], a dual polarized antenna

Manuscript received February 13, 2015; revised September 30, 2015; accepted October 03, 2015. Date of publication October 13, 2015; date of current version November 25, 2015. This work was supported by China Scholarship Council.

C. Gu, S. Gao, Q. Luo, M. Sobhy, and B. Sanz-Izquierdo are with the School of Engineering and Digital Arts, University of Kent, Canterbury CT2 7NT, U.K. (e-mail: cg342@kent.ac.uk; s.gao@kent.ac.uk).

H. Liu is with China Aerospace Science and Technology Corporation, Beijing 100094, China.

T.-H. Loh is with the National Physical Laboratory, Middlesex TW11 0LW, U.K.

J. Li, G. Wei, J. Xu, and F. Qin are with the School of Electronic and Information, Northwestern Polytechnical University, Xi'an 710072, China.

R. A. Abd-Alhameed is with the School of Electrical Engineering and Computer Science, University of Bradford, West Yorkshire BD7 1DP, U.K.

Color versions of one or more of the figures in this paper are available online at http://ieeexplore.ieee.org.

Digital Object Identifier 10.1109/TAP.2015.2490239

with pattern diversity was proposed to achieve four different kinds of linear polarizations using four different ports. The pattern diversity is achieved by switching the antenna radiation pattern between a broadside beam and a conical beam. It is worth noting that the radiation patterns of the antennas presented in [3] and [20] cannot be steered electronically. In [21], a frequency, radiation pattern, and polarization reconfigurable antenna was introduced using a parasitic pixel layer incorporating 60 PIN diodes. The pixel layer consists of a large number of RF switches and chokes, which can deteriorate the antenna performance to some extent. On the other hand, the ESPAR antennas in [8]–[12] are vertically linearly polarized and their polarizations cannot be changed. In [22], a beam steerable loop antenna was presented with four separate tilted beams. Four separate ports were used to generate four different beams, which increases beamforming complexity when used in beam steering applications. Moreover, the polarization of the antenna cannot be altered.

To the best of the author's knowledge, few solutions for antennas with both reconfigurable polarizations and reconfigurable patterns are available in the literature. For wireless systems, it is necessary to optimize both the polarization and radiation patterns of an antenna. The aim of this work is to fill the gap by proposing a novel smart antenna, which achieves both electronic beam switching and reconfigurable polarizations. Thus, the wireless communication system using this antenna can benefit from both the polarization diversity and pattern diversity.

This paper is organized as follows. Section II explains the concept of the polarization and beam reconfiguration using a dual port microstrip antenna surrounded by parasitic elements. Section III describes the detailed design of the antenna and its reconfiguration. Both simulated and measured results of the fabricated antenna are presented. Moreover, the comparison between our work and the related art from literature is provided. Finally, conclusion is drawn in Section IV.

## II. Polarization and Beam Reconfiguration Validation

For an ESPAR antenna, the polarization is determined by the driven element and its beam is controlled by the parasitic elements with proper loads. To interpret the concept of polarization and beam reconfiguration, an inset fed microstrip antenna was simulated and measured. As shown in Fig. 1, the driven element used in this work is a dual feed square microstrip patch antenna, whose polarization can be reconfigured as horizontal, vertical, or diagonal. A 100 mm $\times$ 100 mm Rogers RO4003C laminate with dielectric constant of 3.55, loss tangent of 0.0027, and thickness of 1.524 mm is used as substrate. Parasitic elements are mounted around the patch antenna by the vertically placed "pole-pair," which are illustrated in Fig. 1. The dc bias voltages are supplied by these thin metal strips. The size of the inset fed patch is 31 mm $\times$ 31 mm, which is approximately one half of a wavelength within the substrate. The inset depth of the patch antenna is 5 mm. A quarter-wavelength impedance transformer with a microstrip line length $l = 19.5$ mm, width $w = 0.7$ mm is attached to the patch for antenna impedance matching. The size of one arm of the parasitic dipole is 29 mm $\times$ 4 mm. In order to solder the PIN diode, the gap between the two arms is chosen to be 1 mm.

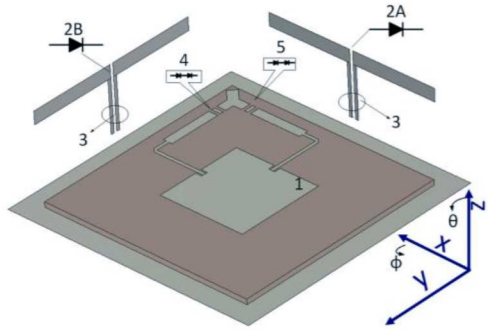


Fig. 1. Structure of the polarization and beam switching reconfigurable antenna. 1: The driven dual-feed patch; 2A, 2B: RPEs: Dipoles incorporating PIN diodes; 3: dc feed lines; 4, 5: Series PIN diode pairs responsible for polarization reconfiguration.

TABLE I
Polarization Direction and PIN Diode Switch Configurations

| | PIN pair - 4 | PIN pair - 5 |
|---|---|---|
| Horizontal-polarization (along x-axis) | F | R |
| Vertical-polarization (along y-axis) | R | F |
| Diagonal-polarization | F | F |

F is forward biased; R is reverse biased.

### A. Polarization Reconfiguration

The dual-port inset fed patch antenna is designed to provide three polarizations for the driven element. Here, the horizontal polarization is defined to be along the x-axis and the vertical polarization is along y-axis. When the PIN diode pair 4 is forward biased and the PIN diode pair 5 is reverse biased, the driven antenna is horizontally polarized. Alternatively, when the PIN diode pair 5 is forward biased and the PIN diode pair 4 is reverse biased, the driven antenna is vertically polarized. Diagonal linear polarization is achieved when the PIN diode pairs 4 and 5 are both forward biased. Hence by controlling the biased states of the PIN diode pairs, the polarizations of the antenna can be electronically reconfigured. Table I below shows the detailed PIN diode switch configurations. The $|S_{11}|$ of the antenna when working at the three polarization states is shown in Fig. 2. As can be seen from the figures, there is only a slight change in $|S_{11}|$ when the antenna is orthogonally polarized, whereas the $|S_{11}|$ of diagonal polarization deteriorates but is still below $-10$ dB.

### B. Beam Reconfiguration

The radiation patterns of the proposed antenna are controlled by the parasitic dipole elements which can be reconfigured either as directors or reflectors. The forward and backward directed beams can be generated by one parasitic element. Thus, more radiation patterns can be generated and the antenna

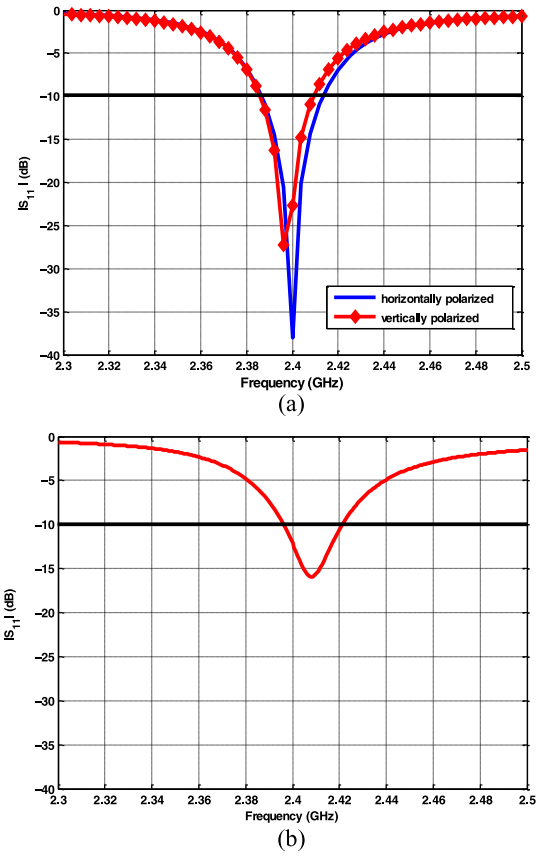


Fig. 2. Measured $S_{11}$ when the antenna in Fig. 1 is (a) orthogonally polarized and (b) diagonally polarized.

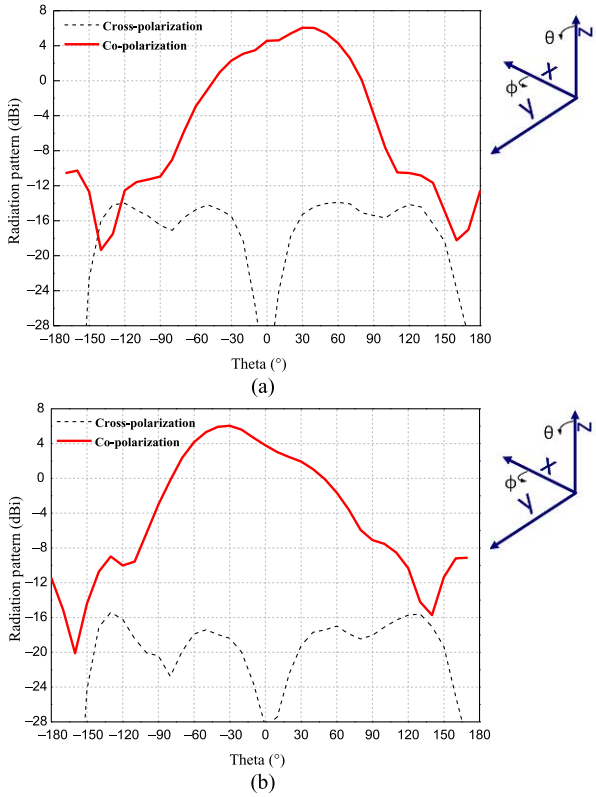


Fig. 3. Measured radiation pattern ($\phi = 90°$) when the antenna given in Fig. 1 is horizontally polarized. (a) Parasitic element (2A) works as a reflector. (b) Parasitic element (2A) works as a director.

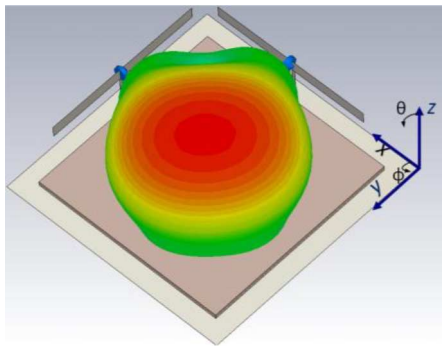

Fig. 4. Simulated radiation pattern when the antenna is diagonally polarized.

beam can be controlled with more freedom if more parasitic elements are used.

The reconfigurable parasitic element (RPE) is composed of a printed dipole and a PIN diode soldered in series between the two halves of the printed dipole. As shown in Fig. 1, the RPEs have dimensions of 60 mm $\times$ 4 mm. The length of an RPE is designed to be approximately a half wavelength at the resonant frequency in dielectric. For a conventional ESPAR antenna, the distance between the driven element and a parasitic element is about quarter-wavelength [7]. Based on this principle, the distance and height between the patch antenna and the RPEs are optimized to generate a tilt beam radiation pattern. It can be seen that the RPEs are placed 45 mm away from the patch center and 25 mm above the ground plane. The PIN diode is controlled by dc voltages supplied through the dc lines. When the PIN diode on the printed dipole is forward or reverse biased, the RPE works as a reflector or a director accordingly.

When the antenna shown in Fig. 1 is horizontally polarized, RPE (2A) is responsible for steering the beam because it is placed along the same direction of the electric field in the patch antenna. Switching the PIN diode changes the electric length of the RPEs, which leads to directing or reflecting the antenna main beam. The measured radiation patterns are given in Fig. 3(a) and (b) with RPE (2A) reconfigured as a reflector and a director, respectively. From Fig. 3, when the RPE works as a reflector, the antenna beam points at an angle of 30°. When the RPE works as a director, the antenna beam points at an angle of $-30°$. The measurement results confirm that the proposed RPE can be altered between a reflector and a director.

When both the PIN diode pairs 4 and 5 in Fig. 1 are forward biased, the patch antenna is diagonally linearly polarized. Due to the surface currents along both edges of the patch, RPEs 2A and 2B can be excited efficiently by electromagnetic coupling. According to the coordinate system shown in Fig. 1, when both the parasitic elements (2A and 2B) are configured as reflectors, the polarization direction is along $\phi = 135°$ and the antenna's three-dimensional (3-D) radiation pattern is shown in Fig. 4.

Fig. 5 shows the radiation pattern of the diagonal polarization and cross-diagonal polarization in $\phi = 135°$ plane. It is noted that the antenna main beam is steered to 35° in the elevation plane and the gains of the copolarization and the cross-polarization are about 5 and $-20$ dBi, respectively.

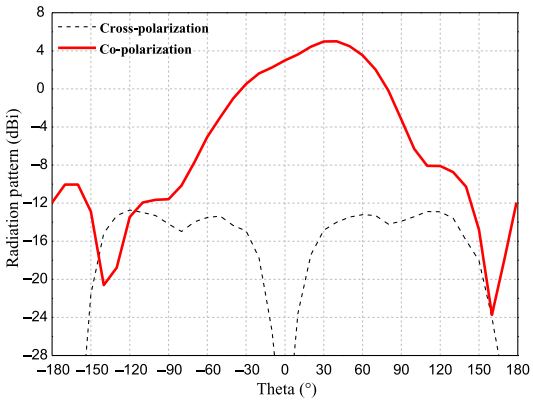


Fig. 5. Measured radiation pattern in $\phi = 135°$ plane.

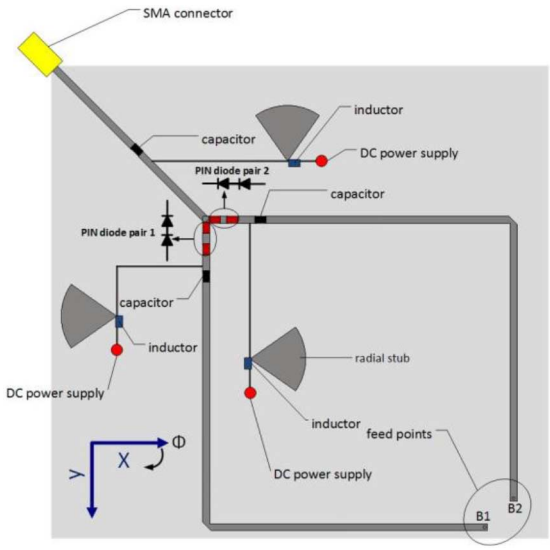


Fig. 6. Schematic drawing of the antenna feed network.

TABLE II
POLARIZATION DIRECTION AND PIN DIODE SWITCH CONFIGURATIONS

| | PIN pair - 1 | PIN pair - 2 |
|---|---|---|
| Horizontal-polarization (along x-axis) | F | R |
| Vertical-polarization (along y-axis) | R | F |
| Diagonal-polarization | F | F |

F is forward biased; R is reverse biased.

By using more of the RPEs in groups, more radiation patterns can be generated and larger beam tilt angles can be achieved, which is discussed in the next section.

## III. DESIGN AND MEASUREMENT RESULTS OF THE BEAM AND POLARIZATION RECONFIGURABLE ANTENNA

The dual feed microstrip antenna and the RPEs validated in Section-II are used to design the beam switching antenna with reconfigurable polarizations. To keep the antenna compact in size and avoid the unwanted radiation from the feed network, it is feasible to design the dc bias network along with the antenna feed lines under the ground plane. The polarization

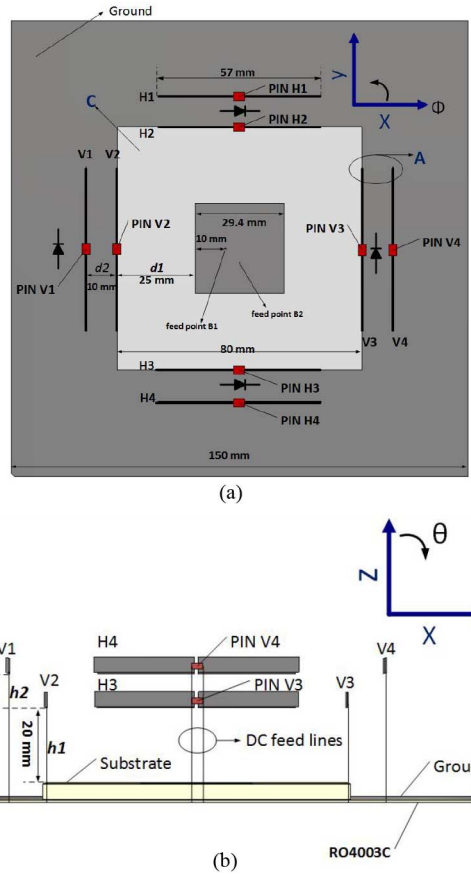


Fig. 7. (a) Plan view (A: parasitic elements, B 1, 2: microstrip antenna feed points, C: substrate). (b) Side view (*h1*: distance fron the patch to the lower parasitic elemet, *h2*: distance fron the the lower parasitic elemet to the upper parasitic element).

of the resulting antenna can be altered between the horizontal and vertical planes by controlling the dc power supply.

### A. Antenna Feed Lines With DC Biasing Network

In order to minimize the spurious radiation raised by the inset fed method and the impact of the feed network, the microstrip antenna is fed by two probes. Thus, the ground plane of the patch antenna can act as a good shield to isolate the unwanted radiation from the dc bias lines. The key to realizing the polarization reconfiguration is to design a two way dc feed line with RF chokes. The detailed feed network is depicted in Fig. 6. From the feed network figure below, three capacitors are used to isolate the dc induced by the two power supply lines. Moreover, quarter-wavelength high impedance lines along with a radial stub are designed to create an ac short circuited point. In order to present high impedance at the design frequency while allowing a dc path for a PIN diode (BAR 64-02V), inductors should be carefully selected as RF chokes. With a self-resonant frequency (SRF) higher than 2.4 GHz, a 56-nH inductor is suitable for this application. After incorporating these components, the two microstrip lines are connected to the probes which feed the patch. The substrate used for the antenna feed network is Rogers RO4003C with a thickness of 0.508 mm. To realize

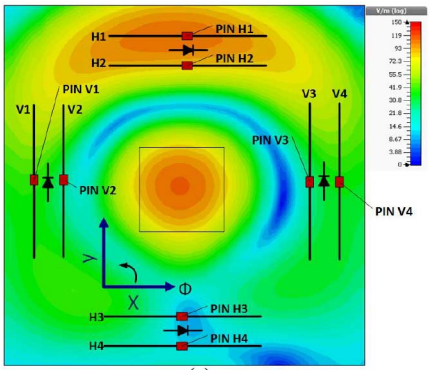


(a)

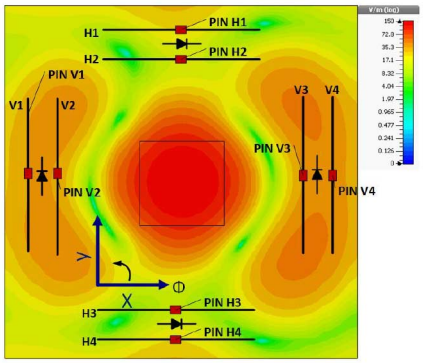


(b)

Fig. 8. Simulated E-field distribution when (a) Beam 1 and (b) Beam 3 is generated at 2.4 GHz.

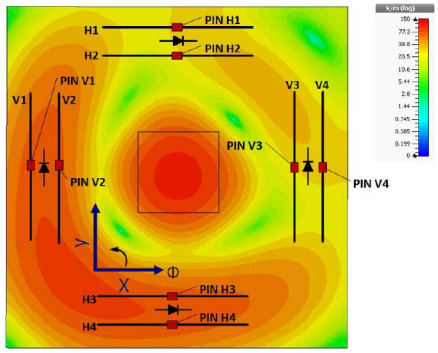


(a)

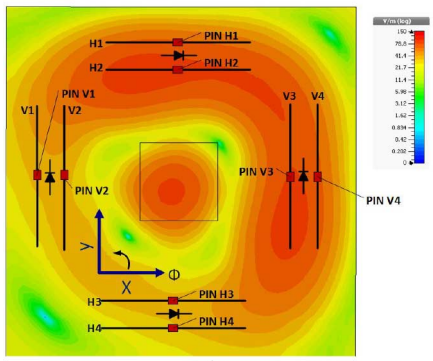


(b)

Fig. 9. Simulated E-field distribution when (a) Beam 4 and (b) Beam 5 is generated at 2.4 GHz.

TABLE III
BEAM AND PIN DIODE SWITCH CONFIGURATIONS (ORTHOGONAL POLARIZATIONS)

| | PIN_H1 H2 | PIN_H3 H4 | PIN_V1/V2/ V3/V4 |
|---|---|---|---|
| Beam 1 ($\phi = 90°$) | R | F | R |
| Beam 2 ($\phi = -90°$) | F | R | R |
| Beam 3 ($\phi = 0°, 180°$) | F | F | R |

F is forward biased 3V; R is reverse biased −3V

TABLE IV
BEAM AND PIN DIODE CONFIGURATIONS (DIAGONAL POLARIZATIONS)

| Beam direction | PIN_H1/H2 | PIN_H3/H4 | PIN_V1/V2 | PIN_V3/V4 |
|---|---|---|---|---|
| $\phi = -135°$ (Beam 4) | F | R | R | F |
| $\phi = 45°$ (Beam 5) | R | F | F | R |

F is forward biased 3V; R is reverse biased −3V

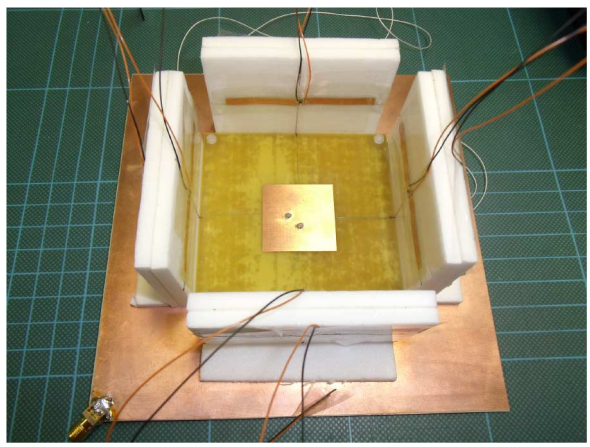

Fig. 10. Fabricated antenna prototype.

higher isolation between the two ports, two series PIN diodes are used for each feed line.

### *B. Antenna Operation Principle*

*1) Polarization Reconfiguration:* The presented antenna can switch its polarization between two orthogonal polarizations and one diagonal polarization, which is realized by the reconfigurable feed network mentioned above. Similar to the operation principle of the antenna in Section II, by independently controlling the PIN diode pairs 1 and 2 in Fig. 6, the feed points B1 and B2 are selected accordingly and thus the polarization of the antenna will be switched. Table II shows the PIN diode switch configurations under which the three polarizations can be obtained.

*2) Beam Reconfiguration:* Based on the validation in Section II, eight reconfigurable parasitic dipoles are employed to realize the beam-switching concept in which four of them are responsible for each polarization. The purpose of introducing the two-layer parasitic dipoles is to generate more beams and a

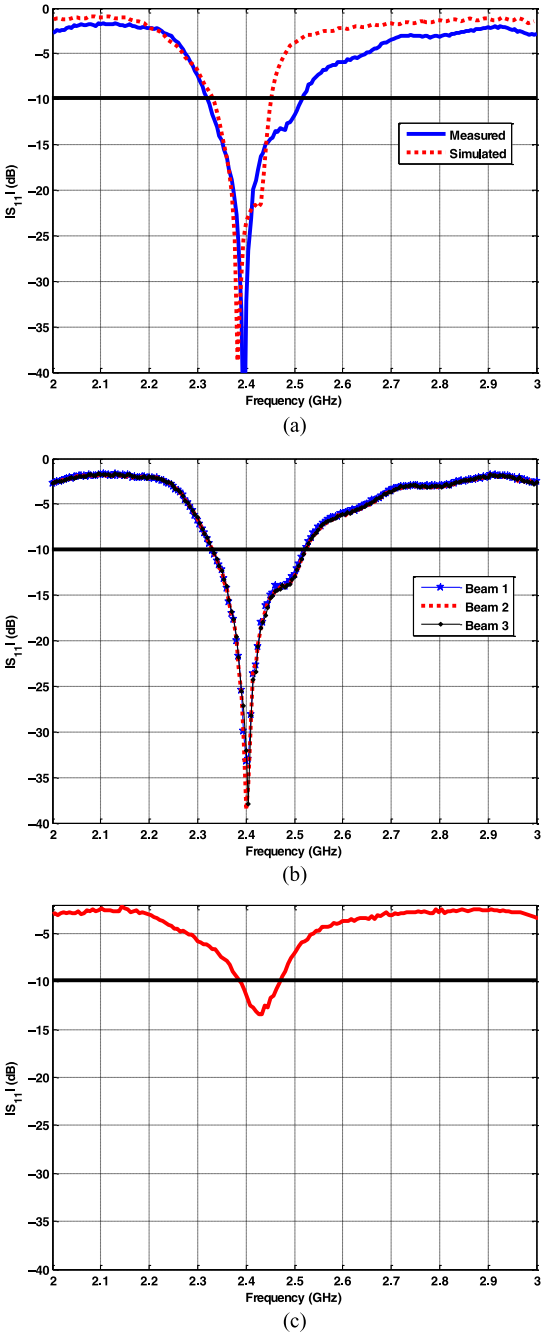


Fig. 11. Measured $S_{11}$ of the fabricated antenna: (a) without eight parasitic elements; (b) when the three beams are generated, respectivley; (c) with diagonal polarization.

larger beam tilt angle. The resulting antenna plan and side view are shown in Fig. 7.

According to Fig. 7(a), the direction along the X-axis is defined as the horizontal polarization and the direction along the Y-axis is defined as the vertical polarization. When explaining the PIN diode switch configurations associated with the beam directions, only the case of horizontal polarization (feed point B1 is excited) is used to illustrate the antenna beam switching mechanism. Due to the symmetry of the antenna structure, the same beam switching property when the antenna is vertically polarized is expected. In this design, three beams

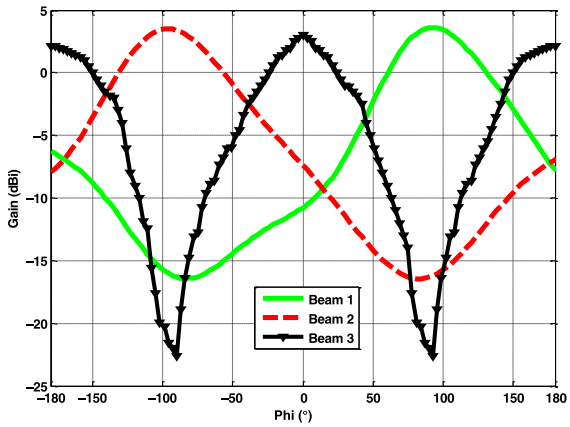


Fig. 12. Measured results of the three beams in $\theta = 45°$ plane.

are generated to steer around the Z-axis with an elevation angle of 45°. As shown in Fig. 7(a), when the horizontal polarization is excited, dipoles H1, H2, H3, and H4 are placed along the polarization direction which means the beam control mainly depends on the configuration of the four PIN diodes in the aforementioned dipoles.

In order to better illustrate the beam switching concept, the simulated E-field distribution at 2.4 GHz when the antenna is horizontally polarized is shown in Fig. 8. Table III shows the detailed PIN diode switch configurations under which the three beams are obtained.

Fig. 8(a) shows the E-field distribution when Beam 1 is generated. It can be seen that dipoles H1, H2, H3, and H4 are responsible for the antenna beam control since they are placed along the polarization direction while the other dipoles have no effect on the beam. According to the E-field distribution of Beam 1, dipoles H1 and H2 work as directors while dipoles H3 and H4 work as reflectors. Due to the symmetrical structure of the antenna, same E-field distribution is expected in the reverse direction when Beam 2 is selected. From Fig. 8(b), it can be seen that Beam 3 is obtained when dipoles V1, V2, V3, and V4 are configured as directors.

Fig. 9 shows the simulated E-field distribution of Beams 4 and 5 when the antenna switches to two diagonal polarizations. With this configuration, the PIN diode pairs 1 and 2 in Fig. 9 are both forward biased. The two beams are generated along the diagonal line of the patch with an elevation angle of 45°. The detailed beam directions and PIN diode switch combinations are given in Table IV.

In Fig. 9(a), as explained in Section II, dipoles V1, V2 and H3, H4, working as directors, are used to steer the main beam. In this case, Beam 4 is steered to $\phi = -135°$. Similarly, Beam 5 is steered to $\phi = 45°$ when the PIN diode pairs are reverse biased, as can be seen in Fig. 9(b).

### C. Measurement Results

The driven element of the designed antenna was fabricated on 4-mm-thick FR-4 with a dielectric constant of 4.4 and a loss tangent of 0.025. The eight parasitic dipoles were printed on Mylar with a dielectric constant of 3 and a thickness of

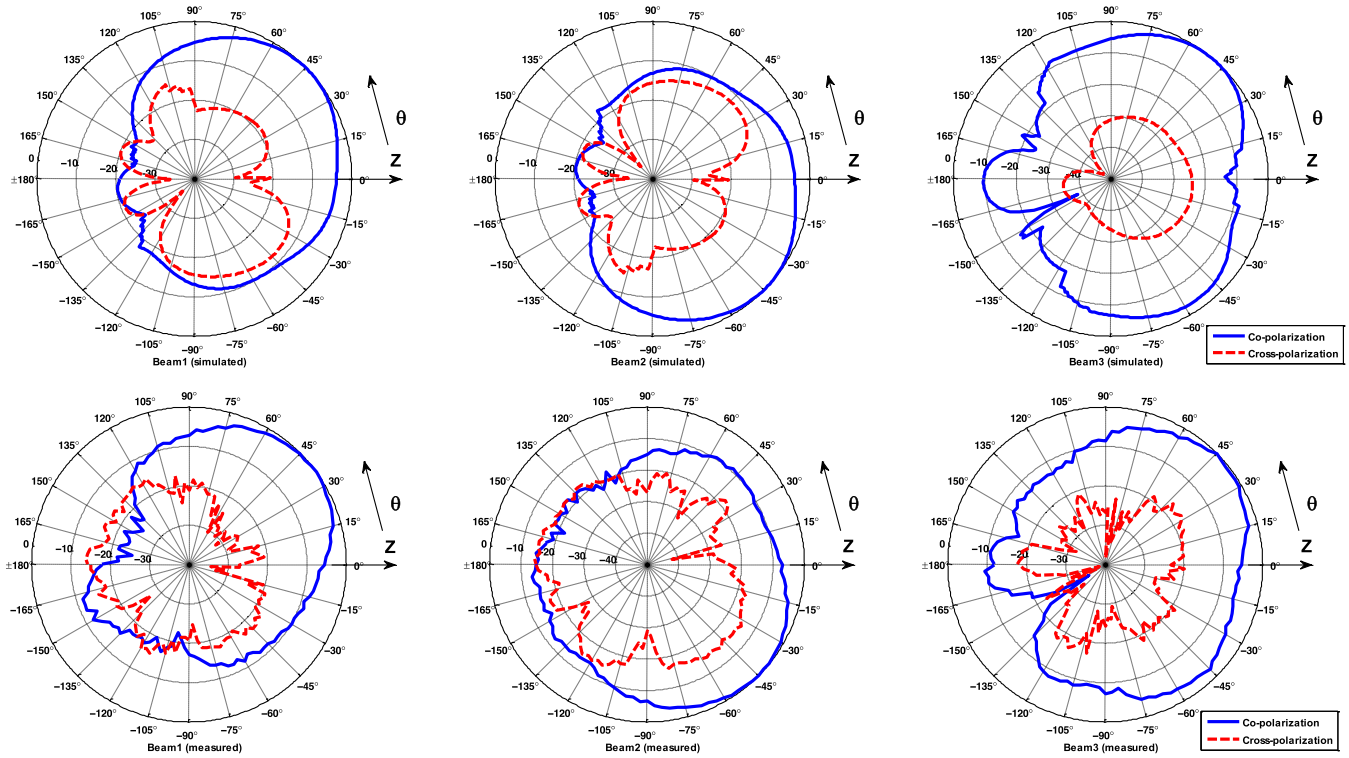


Fig. 13. Simulated and measured radiation patterns in $\phi = 90°$ (Beams 1 and 2) and $\phi = 0°$ (Beam 3) plane.

0.05 mm. The sizes of the patch and dipoles are depicted in Fig. 7. It is noted that the distance $d_1$ and height $h_1$ from patch to dipoles, and the relative distance $d_2$, $h_2$ between dipoles are the main parameters to tune the antenna radiation patterns. The antenna $|S_{11}|$ and radiation patterns are optimized using full-wave simulation software CST Microwave Studio [23]. The fabricated prototype in Fig. 10 is designed to operate in the wireless local area network (WLAN) frequency band.

The simulated and measured S parameters are shown in Fig. 11. The $|S_{11}|$ of the microstrip patch antenna without the eight parasitic elements is shown in Fig. 11(a). It can be seen that when the antenna is horizontally polarized, there is unexpected bandwidth increment of measured $|S_{11}|$, which is caused by incorporating the PIN diodes into the feed network. From Fig. 11(b), it is noted that after switching the eight reconfigurable dipoles, the antenna impedance matching almost remains the same. When the antenna switches to diagonal polarization, the resonate frequency of measured $|S_{11}|$ has shifted upward by about 25 MHz with a magnitude of $-12$ dB at 2.4 GHz, which agrees with the trend of the measured results in Section II.

The beam of the microstrip antenna is steered by the eight parasitic elements with different combinations of PIN diode ON/OFF states. Compared with the beam tilt angle of the validated antenna in Section II, the resulting antenna has a larger beam tilt angle of 45°.

Fig. 12 shows the measured radiation patterns of the three steered beams in $\theta = 45°$ plane when the antenna is horizontally polarized (along X-axis). It is worth noting that Beams 1 and 2 are single-direction beams pointing at 90° and $-90°$, respectively. Beam 3 is a dual-direction beam pointing at 0° and 180° simultaneously. Thus, the antenna beam is able to cover the horizontal plane with three beams with an increment of 90°.

Fig. 13 shows the simulated and measured radiation patterns of Beam 1, Beam 2 in $\varphi = 90°$ plane and beam 3 in $\varphi = 0°$ plane according to the coordinate system in Fig. 7. It can be seen from Fig. 13, the antenna's main beam is steered to 45° in the elevation plane for all the three beams. In addition, the cross-polarizations of the three beams are at least 15 dB less than the copolarizations.

Fig. 14 shows the measured radiation patterns of Beams 4 and 5 in $\theta = 45°$ plane when the antenna is diagonally polarized. The radiation patterns in $\phi = 45°$ plane are shown in Fig. 15, which exhibits the symmetry to the Z-axis. The two beams are both steered to the elevation angle of 45° with cross-polarizations about 22 dB less than copolarizations.

The measured results shown in Figs. 12–15 prove that the proposed antenna's beams can be switched between five different beams, for each polarization.

### *D. Discussion*

From the measured results in Figs. 12 and 14, the antenna realized gain of all the five beams is between 2.5 and 3.5 dBi. These values are less than the validation results in Section II when Rogers RO4003C substrate is used. The main reason for the low efficiency is the high loss (loss tangent $= 0.025$) of the 4-mm-thick FR-4 substrate at the antenna operating frequency. The patch antenna standalone was measured and the radiation efficiency is about 62%. Other factors need to be taken into consideration are the loss of the PIN diodes and the mismatching from the feed network. In antenna feed lines, there are two

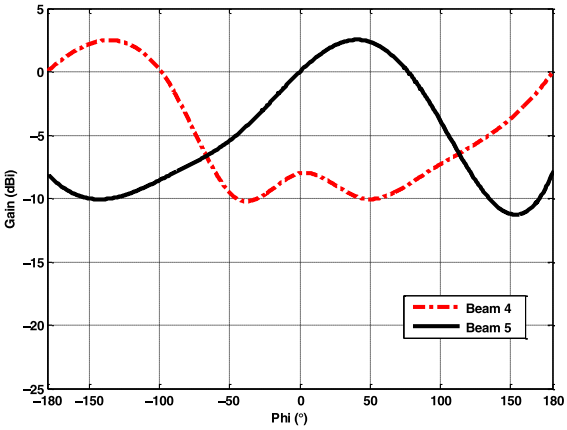


Fig. 14. Measured radiation patterns in $\theta = 45°$ plane.

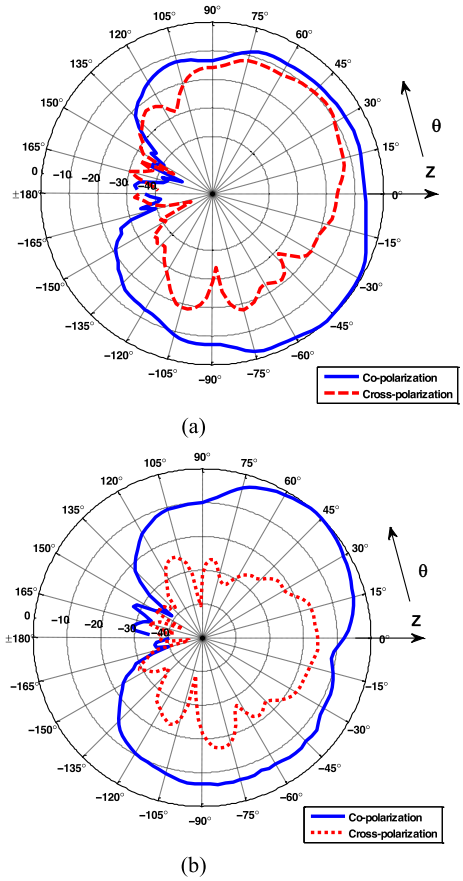


Fig. 15. Measured radiation patterns in $\phi = 45°$ plane: (a) Beam 4 and (b) Beam 5.

diodes working for orthogonal polarization and four diodes for diagonal polarization. Since the loss of a PIN diode is 0.3 dB when it is switched ON, the whole loss of the PIN diodes from the feed network is larger than 0.6 dB. Moreover, on each of the parasitic dipole elements, one diode is used which can contribute loss to the overall antenna. After incorporating the feed network and the parasitic elements, the radiation efficiency further reduces to 45.7% for orthogonal polarization and 36.3% for diagonal polarization. Table V shows the comparison of the various polarization or beam reconfigurable antennas from the literature.

TABLE V
COMPARISON BETWEEN CITED WORKS AND OUR WORK

| Ref no. | Polarization reconfigurable | Beam reconfigurable | Gain (dBi) | Efficiency |
|---|---|---|---|---|
| [7], [12] | No | Yes | 6–7 | ≥ 70% |
| [13] | Yes | No | 5 | Not given |
| [14] | Yes | No | ≤3 | Not given |
| [15] | Yes | No | ≤0.15 | Not given |
| [16] | Yes | No | 4.2–8.45 | Not given |
| [22] | No | Yes | 7.3–9.3 | Not given |
| Our work | Yes | Yes | 2.5–3.5 | 36.3–45.7% |

To combat multipath fading, orthogonal frequency division multiplexing (OFDM) is adopted in current wireless systems to guarantee that the delay spread is much smaller than a symbol period so that the multipath components will be combined together and treated as one path. Generally, in wireless systems, pilot symbols are used to measure the channel gain. In the presented design, up to eight beams with different polarizations are generated. The signal strength measurement takes less than 80 ns since the PIN diode switching time is less than 10 ns. It is short enough for a practical wireless system to measure the signal strength of all the beams. Based on the measurement results, the beam and polarization are selected with the highest signal strength.

## IV. CONCLUSION

A novel compact-size, low-cost smart antenna with electronically switchable radiation patterns and reconfigurable polarizations is presented in this paper. The measurement proved that the antenna can have its polarizations dynamically altered to realize orthogonal or diagonal linear polarizations. By switching the bias voltage over the PIN diodes, the antenna radiation patterns can be switched between five beams at each polarization.

The pattern diversity generated by switching parasitic elements instead of switching feeders [24] makes this antenna suitable for multiple-input multiple-output (MIMO) systems in terms of conquering the multipath fading effects and cochannel interferences. Furthermore, the RPEs provide more freedom for designers to control the antenna radiation patterns.

## REFERENCES

[1] S. Gao, A. Sambell, and S. S. Zhong, "Polarization-agile antennas," *IEEE Antennas Propag. Mag.*, vol. 48, no. 3, pp. 28–37, Jun. 2006.
[2] F. Ferrero *et al.*, "A novel quad-polarization agile patch antenna," *IEEE Trans. Antennas Propag.*, vol. 57, no. 5, pp. 1563–1567, May 2009.
[3] H. T. Chattha *et al.*, "Polarization and pattern diversity-based dual-feed planar inverted-F antenna," *IEEE Trans. Antennas Propag.*, vol. 60, no. 3, pp. 1532–1539, Mar. 2012.
[4] R. Jeen-Sheen and S. Chuang-Jiashih, "Polarization-diversity ring slot antenna with frequency agility," *IEEE Trans. Antennas Propag.*, vol. 60, no. 8, pp. 3953–3957, Aug. 2012.
[5] R. Jeen-Sheen and H. Ming-Jyun, "Design of polarization diversity patch antenna based on a compact reconfigurable feeding network," *IEEE Trans. Antennas Propag.*, vol. 62, no. 10, pp. 5349–5352, Oct. 2014.

[6] R. F. Harrington, "Reactively controlled directive arrays," *IEEE Trans. Antennas Propag.*, vol. 26, no. 3, pp. 390–395, May 1978.
[7] R. Schlub, J. W. Lu, and T. Ohira, "Seven-element ground skirt monopole ESPAR antenna design from a genetic algorithm and the finite element method," *IEEE Trans. Antennas Propag.*, vol. 51, no. 11, pp. 3033–3039, Nov. 2003.
[8] C. Sun, "Smart antennas for 3G and future wireless communications: Algorithms and implementations," Ph.D. dissertation, Nanyang Technological University, Singapore, 2005.
[9] H. T. Liu, S. Gao, and T. H. Loh, "Compact dual-band antenna with electronic beam-steering and beamforming capability," *IEEE Antennas Wireless Propag. Lett.*, vol. 10, pp. 1349–1352, Dec. 2011.
[10] H. T. Liu, S. Gao, and T. H. Loh, "Low-cost beam-switching circularly-polarised antenna using tunable high impedance surface," in *Proc. Loughborough Antennas Propag. Conf. (LAPC)*, Apr. 2010, pp. 1–4.
[11] H. T. Liu, S. Gao, and T. H. Loh, "Electrically small and low cost smart antenna for wireless communication," *IEEE Trans. Antennas Propag.*, vol. 60, no. 3, pp. 1540–1549, Mar. 2012.
[12] C. Gu *et al.*, "Design of broadband ESPAR antenna using inverted F monopoles," in *Proc. 8th Eur. Conf. Antennas Propag. (EuCAP)*, Apr. 2014, pp. 1814–1817.
[13] Y. F. Wu *et al.*, "A reconfigurable quadri-polarization diversity aperture-coupled patch antenna," *IEEE Trans. Antennas Propag.*, vol. 55, no. 3, pp. 1009–1012, Mar. 2007.
[14] Y. Li *et al.*, "Polarization reconfigurable slot antenna with a novel compact CPW-to-slotline transition for WLAN application," *IEEE Antennas Wireless Propag. Lett.*, vol. 9, pp. 252–255, Apr. 2010.
[15] B. Li and Q. Xue, "Polarization-reconfigurable omnidirectional antenna combining dipole and loop radiators," *IEEE Antennas Wireless Propag. Lett.*, vol. 12, pp. 1102–1105, Sep. 2013.
[16] P. Y. Qin, Y. J. Guo, and C. Ding, "A dual-band polarization reconfigurable antenna for WLAN systems," *IEEE Trans. Antennas Propag.*, vol. 61, no. 11, pp. 5706–5713, Nov. 2013.
[17] S. Gao *et al.*, "A broad-band dual-polarized microstrip patch antenna with aperture coupling," *IEEE Trans. Antennas Propag.*, vol. 51, no. 4, pp. 898–900, Apr. 2003.
[18] S. C. Gao *et al.*, "Dual-polarized, slot-coupled, planar antenna with wide bandwidth," *IEEE Trans. Antennas Propag.*, vol. 51, no. 3, pp. 441–448, Mar. 2003.
[19] S. Gao and A. Sambell, "Dual-polarized broad-band microstrip antennas fed by proximity coupling," *IEEE Trans. Antennas Propag.*, vol. 53, no. 1, pp. 526–530, Jan. 2005.
[20] S. L. S. Yang *et al.*, "A dual-polarized antenna with pattern diversity," *IEEE Antennas Propag. Mag.*, vol. 50, no. 6, pp. 71–79, Dec. 2008.
[21] D. Rodrigo, B. A. Cetiner, and L. Jofre, "Frequency, radiation pattern and polarization reconfigurable antenna using a parasitic pixel layer," *IEEE Trans. Antennas Propag.*, vol. 62, no. 6, pp. 3422–3427, Jun. 2014.
[22] A. Pal *et al.*, "Dual-band low-profile capacitively coupled beam-steerable square-loop antenna," *IEEE Trans. Antennas Propag.*, vol. 62, no. 3, pp. 1204–1211, Mar. 2014.
[23] CST Microwave Studio. (2014). [Online]. Available: www.cst.com.
[24] Y. Li *et al.*, "Experimental analysis of a wideband pattern diversity antenna with compact reconfigurable CPW-to-slotline transition feed," *IEEE Trans. Antennas Propag.*, vol. 59, no. 11, pp. 4222–4228, Nov. 2011.

**Chao Gu** received the B.S. and M.S. degrees in electronic engineering from Xidian University, Xi'an, China, in 2009 and 2012, respectively. He is working toward the Ph.D. degree in electronic engineering at University of Kent, Canterbury, U.K.

His research interests include smart antennas, reconfigurable antennas, and frequency selective surfaces.

**Steven (Shichang) Gao** received the Ph.D. degree in microwave engineering from Shanghai University, Shanghai, China.

He is a Professor and Chair in RF and Microwave Engineering at the University of Kent, Canterbury, U.K. His research interests include smart antennas, phased arrays, satellite antennas, RF/microwave/mm-wave circuits, satellite communications, mobile communications, and radars.

**Haitao Liu** received the Ph.D. degree from the University of Surrey, Guildford, Surrey, U.K., in 2012.

He is currently with China Aerospace Science and Technology Corporation, Beijing, China.

**Qi Luo** received the Ph.D. degree in electrical and computer engineering from the University of Porto, Portugal, in 2012.

He is currently a Research Associate with the University of Kent, Canterbury, U.K.

**Tian-Hong Loh** is with National Physical Laboratory, Middlesex, U.K.

**Mohammed Sobhy** is currently an Emeritus Professor with the University of Kent, Canterbury, U.K.

**Jianzhou Li** is an Associate Professor with the Northwestern Polytechnical University, Xi'an, China.

**Gao Wei** is a Professor with the Northwestern Polytechnical University, Xi'an, China.

**Jiadong Xu** is a Professor with the Northwestern Polytechnical University, Xi'an, China.

**Fan Qin** is currently working toward the Ph.D. degree at the Northwestern Polytechnical University, Xi'an, China.

**Benito Sanz-Izquierdo** is a Lecturer with the University of Kent, Canterbury, U.K.

**Raed A. Abd-Alhameed** is a Professor with the University of Bradford, Bradford, U.K.